Electrochemistry Communications 26 (2013) 37–40

Contents lists available at SciVerse ScienceDirect

Electrochemistry Communications

journal homepage: www.elsevier.com/locate/elecom

Selective anion exchange membranes for high coulombic efficiency vanadium redox flow batteries

Dongyang Chen [a], Michael A. Hickner [a,*], Ertan Agar [b], E. Caglan Kumbur [b,**]

[a] Department of Materials Science and Engineering, The Pennsylvania State University, University Park, PA 16802, USA
[b] Electrochemical Energy Systems Laboratory, Department of Mechanical Engineering and Mechanics, Drexel University, Philadelphia, PA 19104, USA

ARTICLE INFO

Article history:
Received 14 September 2012
Received in revised form 28 September 2012
Accepted 2 October 2012
Available online 8 October 2012

Keywords:
Anion exchange membrane
Capacity fade
Coulombic efficiency
Self-discharge
Vanadium redox flow battery

ABSTRACT

A quaternary ammonium functionalized poly(fluorenyl ether) anion exchange membrane (AEM) with extremely low VO^{2+} permeation was characterized for vanadium redox flow battery (VRFB) application. One hundred percent coulombic efficiency (CE) was achieved for the AEM-based VRFB at all the current densities tested. Comparatively, the CE of a N212 membrane-based VRFB was lower than 94% and varied with charge/discharge current density. At current densities lower than 60 mA cm^{-2}, the energy effiency of the AEM-based VRFB was higher than that of a device with N212. The cycling performance demonstrated that the AEM-based VRFB was free of capacity fade, which is a consequence of its low VO^{2+} permeability. These observations are of significant importance for flow batteries that operate intermittently or at moderate current densities.

© 2012 Elsevier B.V. All rights reserved.

1. Introduction

As a promising technology for large-scale stationary energy storage, vanadium redox flow batteries (VRFBs) have experienced several significant improvements in cell design [1], modeling [2], and electrode materials [3]. The acceleration of VRFB technology is especially evident when considering innovations in the electrode/electrolyte separator which isolates the anolyte and catholyte compartments while maintaining charge transport across the cell [4–6]. The majority of current research on VRFB separators is aimed at developing proton exchange membranes (PEMs) that feature high proton conductivity, low vanadium permeability, and long lifetime. VRFBs with over 99% coulombic efficiency (CE) were obtained by strategic tuning of the membrane's chemical structure and properties [7]; however, the capacity fade of these batteries due to vanadium crossover cannot be ignored. Nanofiltration membranes that selectively transfer protons compared to vanadium ions by size exclusion were proposed for VRFBs to achieve 98% CE [8]. While these membranes have advantages for high performance cells, it would be highly desirable to have a zero capacity fade device.

Anion exchange membranes (AEMs) block the transport of cations due to Donnan repulsion effects and are widely used in electrodialysis [9]. Preliminary evaluations of AEMs in VRFBs were reported with CEs of as high as 99%; however, limited information was given regarding the transport relationships by which AEMs operate in VRFBs and how the basic properties of the membrane contributed to high performance in devices [10,11]. It is generally recognized that protons are the charge carriers passing through the separator of VRFBs. In fact, any ion, such as sulfate in a sulfuric acid-based electrolyte, can be the charge carrier to balance the redox reactions of the vanadium species. This inspired us to explore the properties of AEMs to prevent vanadium crossover and capacity fade in VRFBs. Herein, we report our recent success in employing an anion exchange membrane in VRFB to obtain 100% CE under various current densities.

2. Experimental

Quaternary ammonium functionalized poly(fluorenyl ether) (QA-PFE) with an ion exchange capacity of 2.0 mequiv. g^{-1} was synthesized [12]. Its chemical structure is shown in Scheme 1. This QA-PFE was in I^- counter-ion form as synthesized and its intrinsic viscosity was 0.65 g dL^{-1}. The QA-PFE anion exchange membrane (AEM) was cast from 8 wt.% solution in N,N′-dimethylacetamide on a glass plate at 80 °C under atmospheric pressure for 24 h. The AEM was ion-exchanged to the SO_4^- anion in 1 M Na_2SO_4 for 24 h, and then immersed in deionized water for 24 h with three water exchanges. The 56 μm thick AEM was used for performance evaluation in a VRFB. Nafion® N212 (Ion Power Inc., USA) was examined under the same conditions.

Ionic conductivity was measured by two-probe electrochemical impedance spectroscopy (EIS) using a Solartron 1260A frequency response analyzer [13]. The VO^{2+} permeability measurements were conducted in a membrane-separated cell using the standard procedure from literature

* Corresponding author. Tel.: +1 814 867 1847; fax: +1 814 865 2917.
** Corresponding author. Tel.: +1 215 895 5871; fax: +1 215 895 1478.
E-mail addresses: hickner@matse.psu.edu (M.A. Hickner), eck32@drexel.edu (E.C. Kumbur).

1388-2481/$ – see front matter © 2012 Elsevier B.V. All rights reserved.
http://dx.doi.org/10.1016/j.elecom.2012.10.007

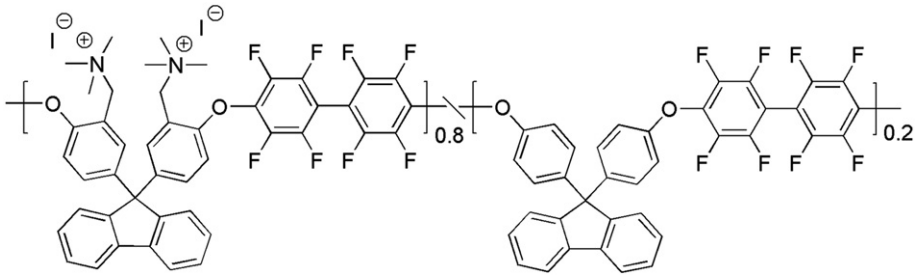

Scheme 1. Chemical structure of QA-PFE.

[7]. VRFB performance measurements were conducted with 100 mL of 1 M $VOSO_4$ + 2.5 M H_2SO_4 solution as the positive electrolyte and 50 mL of 1 M $VOSO_4$ + 2.5 M H_2SO_4 solution as the negative electrolyte. The cell configuration was the same as our previous report [14]. The cell was first charged to 1.7 V and discharged to 0.7 V at 80 mA cm^{-2}, and then cycled at this current density for 15 cycles and finally charged-discharged at 60, 40 and 20 mA cm^{-2} with pre-discharging at the corresponding current density before the final charging–discharging process. The coulombic efficiency (CE), voltage efficiency (VE) and energy efficiency (EE) for any galvanostatic charging–discharging process were calculated from:

$$CE = \frac{t_d}{t_c} \times 100\% \quad (1)$$

$$VE = \frac{V_d}{V_c} \times 100\% \quad (2)$$

$$EE = CE \times VE \quad (3)$$

where t_d is the discharging time, t_c is the charging time, V_d is the average discharging voltage, V_c is the average charging voltage.

3. Results and discussion

3.1. Ion conductivity and vanadium permeability of AEMs

AEMs are notorious for their low conductivity compared to PEMs due to the low mobility anions compared to protons in aqueous solution. The proton conductivity of N212 at room temperature was 69 mS cm^{-1} while the SO_4^{2-} conductivity of our AEM at room temperature was only 5 mS cm^{-1}. Fortunately, the high concentration of SO_4^{2-} in the electrolytes of VRFBs mitigates the low conductivity of AEMs due to uptake of free SO_4^{-} ions into the membrane. Furthermore, the existence of protons in the anolyte and catholyte may also help lower the resistance of AEMs. We measured the conductivity of N212 and the QA-PFE AEM after equilibration in 1 M $VOSO_4$ + 2.5 M H_2SO_4 solution for 24 h. The apparent conductivity of N212 was 44 mS cm^{-1}, lower than its proton conductivity in pure water. The lower conductivity was due to some of the sulfonate sites being occupied by vanadium cations. Also, increased acid concentration has been observed to decrease the conductivity of solutions and membranes [15,16]. The measured conductivity of the AEM in 1 M $VOSO_4$ + 2.5 M H_2SO_4 increased to 20 mS cm^{-1}, almost half of the total ion conductivity of N212.

For N212, the permeation of VO^{2+} could be observed by the change of the vanadium deficient solution from clear to blue within 1 h. The VO^{2+} permeability of N112 was calculated to be 3.2×10^{-12} m^2 s^{-1}, similar to literature values [5]. For the AEM, there was no solution color change after one month and no detectable VO^{2+} ion by UV–vis analysis. This absence of VO^{2+} crossover indicated that the AEM had excellent capability to prevent the transport of vanadium ions. Therefore, we propose that the AEM in a VRFB transports both proton and sulfate ions but retains vanadium ions as depicted in Fig. 1.

3.2. VRFB performance under different current densities

The charge–discharge curves of VRFBs assembled with QA-PFE or N212 membranes at 20 mA cm^{-2} are shown in Fig. 2. The N212-based VRFB had lower charge voltage than the QA-PFE AEM-based VRFB. This difference in charge voltage was attributed to the lower resistance of N212 as discussed above since both membranes had similar thickness. The average discharge voltage for both the VRFBs was similar even though the discharge curve of the N212 VRFB was slightly lower than the discharge curve of the AEM-based VRFB. Since N212 had lower resistance, its VRFB performance was expected to afford higher average discharge voltage than the AEM. Nevertheless, N212 suffered from large vanadium permeation resulting in short-circuit reactions, which negatively affected the discharge voltage and thus offset its lower resistance.

The coulombic efficiency (CE) of the N212-based VRFB at 20 mA cm^{-2} was 81.2%, similar to literature values [17]. Surprisingly, the CE of the QA-PFE AEM VRFB was 100%, or as near to 100% as we could measure, suggesting there was no vanadium crossover or side reactions during cell operation. Generally, the CE of a VRFB is influenced by vanadium permeation, electrode corrosion, and side reactions of vanadium ions with oxygen or other solution contaminants. For our measurements, we kept the upper limit of charging voltage to 1.7 V, which avoids corrosion of the electrodes [18]. Furthermore, a sealed and N_2 purged electrolyte tank eliminated side reactions of vanadium ions. Together, with the undetectable vanadium permeation of our AEM, it is reasonable to achieve 100% CE, which paves the way for very high energy efficiency VRFBs even during long periods of test.

Fig. 3 shows the influence of current density on coulombic efficiency (CE), voltage efficiency (VE) and energy efficiency (EE) of the VRFBs. It can be seen that the AEM-based VRFB achieved 100% CE

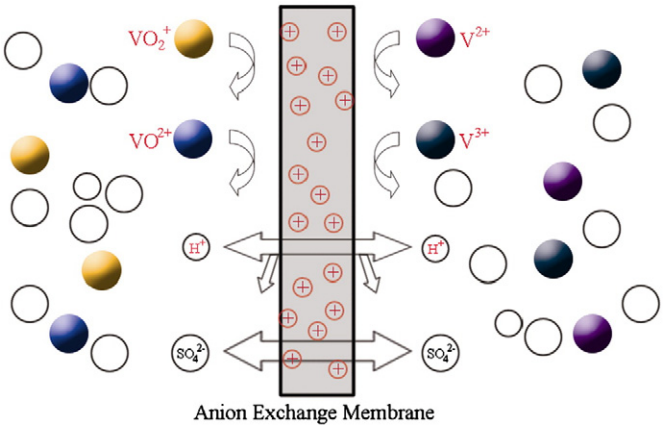

Fig. 1. Functions of an AEM in a VRFB.

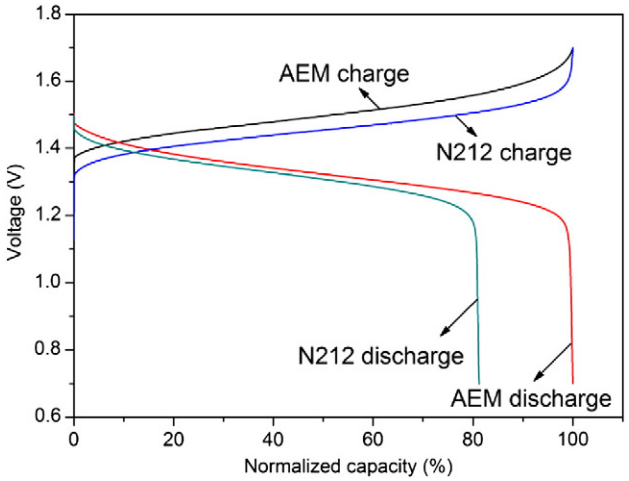

Fig. 2. Charge–discharge curves of VRFBs at 20 mA cm^{-2}.

for all the current densities tested. The CE of the N212-based VRFB increased with increasing current density, which was due to the decreased time allowed for vanadium permeation. The VE of both the VRFBs decreased with the increasing current density because of the higher ohmic polarization at higher current densities. The N212 VRFB had a more pronounced advantage in VE with increasing current density compared to the AEM VRFB, suggesting a larger influence of membrane resistance at higher current densities, as expected. The EE of the AEM VRFB decreased monotonically from 20 mA cm^{-2} to 80 mA cm^{-2} due to the decreasing VE, while the EE of the N212 VRFB exhibited a peak value at 40 mA cm^{-2}. It is worthwhile to mention that the AEM VRFB had higher energy efficiency than the N212 VRFB at current densities lower than 60 mA cm^{-2}, making it highly desirable for moderate current density VRFB operation.

3.3. VRFB cycling performance

Capacity fade and CE change versus cycle number were investigated in VRFB cycling tests (Fig. 4). Capacity fade of the N212-based VRFB was observed, while the QA-PFE-based VRFB showed no measureable capacity fade. This observation correlated well with no vanadium crossover or no self-discharge in the AEM VRFB and was in good agreement with the 100% CE of the battery. The absence of capacity fade has not been met so far in other separator work. The CEs of the VRFBs were very stable during cycling. This phenomenon is typical in flow battery systems as long as there is no materials damage during device operation.

4. Conclusions

A quaternary ammonium functionalized poly(fluorenyl ether) AEM was applied successfully as a VRFB separator. The QA-PFE AEM had low intrinsic anionic conductivity, but upon soaking in VRFB electrolyte solution achieved almost half the conductivity of N212. Furthermore, the AEM VO^{2+} permeation was undetectable for one month. It was found that the QA-PFE AEM-based VRFB achieved 100% coulombic efficiency at all the current densities tested, which has not been reported previously. The energy efficiency of this VRFB was higher than that of a N212 VRFB when the current density was lower than 60 mA cm^{-2}. Capacity fade was observed for the N212-based VRFB while it was absent for the AEM-based VRFB. This work points to new directions for maintenance-free and long-lifetime VRFBs under a variety of operating and rest conditions.

Acknowledgments

The work was supported by the Office of Electricity (OE) Delivery and Energy Reliability, U.S. Department of Energy (DOE) under contract DE-AC05-76RL01830 and the Advanced Research Projects Agency—Energy (ARPA-E), U.S. DOE, under Award No. DE-AR0000121.

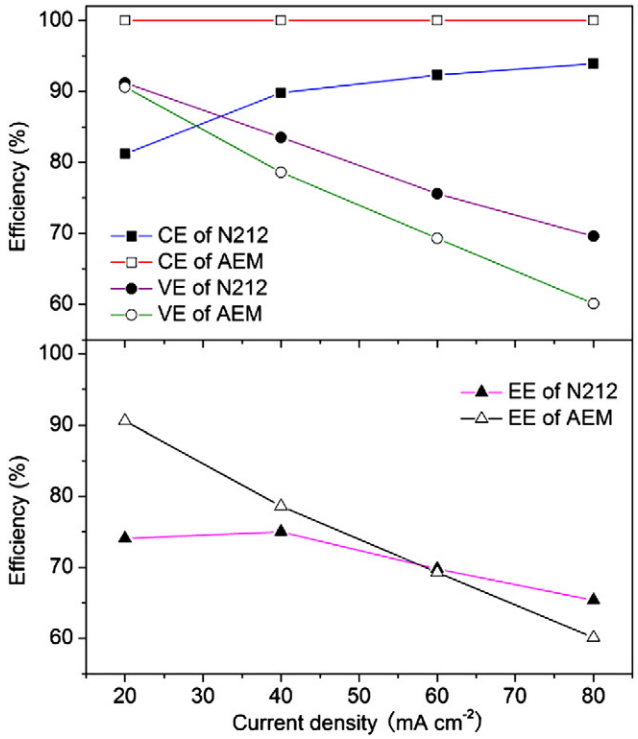

Fig. 3. Coulombic efficiency (CE), voltage efficiency (VE) and energy efficiency (EE) of VRFBs at various current densities.

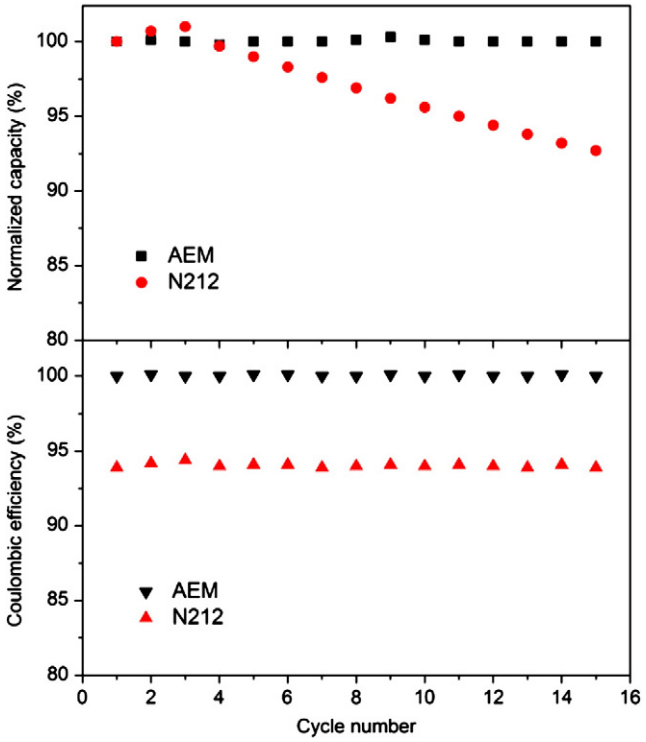

Fig. 4. Normalized capacity changes and coulombic efficiencies of VRFBs in the cyling test.

We also acknowledge the support from the Southern Pennsylvania Ben Franklin Commercialization Institute (Grant No. 001389-002).

References

[1] D.S. Aaron, Q. Liu, Z. Tang, G.M. Grim, A.B. Papandrew, A. Turhan, T.A. Zawodzinski, M.M. Mench, Journal of Power Sources 206 (2012) 450.
[2] K.W. Knehr, E.C. Kumbur, Electrochemistry Communications 23 (2012) 76.
[3] K.J. Kim, M.S. Park, J.H. Kim, U. Hwang, N.J. Lee, G. Jeong, Y.J. Kim, Chemical Communications 48 (2012) 5455.
[4] X. Li, H. Zhang, Z. Mai, H. Zhang, I. Vankelecom, Energy & Environmental Science 4 (2011) 1147.
[5] D. Chen, S. Wang, M. Xiao, Y. Meng, Journal of Power Sources 195 (2010) 2089.
[6] J. Ma, Y. Wang, J. Peng, J. Qiu, L. Xu, J. Li, M. Zhai, Journal of Membrane Science 419–420 (2012) 1.
[7] D. Chen, S. Kim, L. Li, G. Yang, M.A. Hickner, RSC Advances 2 (2012) 8087.
[8] H. Zhang, H. Zhang, X. Li, Z. Mai, W. Wei, Energy & Environmental Science 5 (2012) 6299.
[9] T. Sata, Journal of Membrane Science 167 (2000) 1.
[10] S. Zhang, C. Yin, D. Xing, D. Yang, X. Jian, Journal of Membrane Science 363 (2010) 243.
[11] J. Fang, H. Xu, X. Wei, M. Guo, X. Lu, C. Lan, Y. Zhang, Y. Liu, T. Peng, Polymers for Advanced Technologies (2012), http://dx.doi.org/10.1002/pat.3066.
[12] D. Chen, M.A. Hickner, S. Wang, J. Pan, M. Xiao, Y. Meng, International Journal of Hydrogen Energy (2012), http://dx.doi.org/10.1016/j.ijhydene.2012.08.051.
[13] C.H. Fujimoto, M.A. Hickner, C.J. Cornelius, D.A. Loy, Macromolecules 38 (2005) 5010.
[14] K.W. Knehr, E. Agar, C.R. Dennison, A.R. Kalidindi, E.C. Kumbur, Journal of the Electrochemical Society 159 (2012) A1146.
[15] S.N. Suarez, J.R.P. Jayakody, S.G. Greenbaum, T. Zawodzinski, J.J. Fontanella, The Journal of Physical Chemistry. B 114 (2010) 8941.
[16] Z. Tang, R. Keith, D.S. Aaron, J.S. Lawton, A.P. Papandrew, T.A. Zawodzinski, ECS Transactions 41 (2012) 25.
[17] X. Teng, Y. Zhao, J. Xi, Z. Wu, X. Qiu, L. Chen, Journal of Power Sources 189 (2009) 1240.
[18] H. Liu, Q. Xu, C. Yan, Y. Qiao, Electrochimica Acta 56 (2011) 8783.